



Cite this: *RSC Adv.*, 2020, **10**, 13095

Received 18th November 2019
 Accepted 20th March 2020

DOI: 10.1039/c9ra09599c
rsc.li/rsc-advances

Bead based facile assay for sensitive quantification of native state green fluorescent protein†

Jung Min Kim,^a Baik Lin Seong^{*b} and Dong-Kwon Lim^{ID, *a}

A facile method for the quantification of native state protein is strongly required to accurately determine the amount of expressed protein of interest. Here we report a simple bead-based assay, which can sensitively quantify the amount of native state green fluorescent protein using Ni-NTA (nickel-nitrilotriacetic acid)-modified microbead particles. The bead-based method is simple and straightforward to perform and it showed a highly sensitive capability to detect the expressed fluorescent protein because of the enriched fluorescent protein on the beads.

Introduction

The green fluorescent protein (GFP) has been an attractive tool for the studies of complex biological events in various ways combining with fluorescence microscopy.^{1,2} The recent developments in the use of fluorescent protein has led to a breakthrough technology for the investigations of biological molecules and biologic functions, dynamics, and visualization.^{3–6} The powerful applications of GFP have been relying on the capability of expressing GFP as a marker for a specific protein production. In such cases, the gene is incorporated into the genome of the organism in the region of the DNA that codes for the target proteins.^{7–9}

Once the target proteins with GFP are expressed inside the cells, the production of protein can be identified with fluorescence microscopy. In the purification of expressed fluorescent protein, polyacrylamide gel electrophoresis-based analysis have been previously applied to determine the purity, molecular weight, and the structure of expressed protein.^{10,11} After obtaining the purified fluorescent protein, the amount of GFP can be estimated by measuring the fluorescence intensity. The structural changes of GFP can also be monitored by measuring the fluorescence intensity of GFP solution with urea treatment. However, the overall procedures are complicated and time-consuming.

The detection limit based on the fluorescence intensity of solution state GFP is not so excellent enough to detect the picogram range of GFP solution.¹² To address the limitations, Ni-NTA (nickel-nitrilotriacetic acid) bead based method has

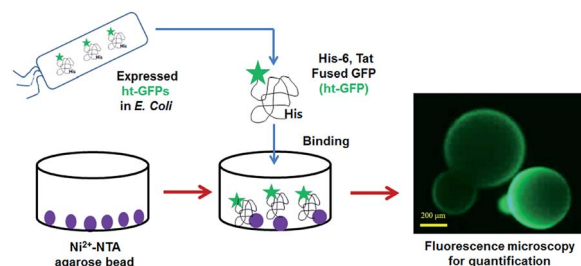
been used to obtain a purified target protein. And a subsequent enzyme-linked immunoassay was applied to quantify the amount of purified target protein. Although performing the enzyme-linked immunosorbent assay can determine the amount of protein, it is a complex and time-consuming procedure.

In this paper, we report the fluorescence-based quantification method for fluorescent protein using Ni-NTA modified microbead particles¹³ without relying on the enzyme-based quantification procedures. The fluorescence signal could be directly measured from the bead after capturing the fluorescent protein through the interaction between Ni-NTA on bead and hexa-histidine (His-6) residue of the target protein.^{14,15} The bead based assay could detect a considerably low concentration of target protein in a native state (Scheme 1).

Experiment

Materials

Ni-NTA-agarose beads (pore size 45–165 µm)^{14,16} were purchased from Thermo Fisher Scientific (Waltham, MA, USA) and Dynabeads® TALON™ magnetic beads (pore size 1.0 µm)¹⁷ were purchased from Clontech Laboratories Inc. (Mountain View,



Scheme 1 Bead-based assay to quantify the amount of expressed ht-GFPs (hexa-histidine and Tat fused green fluorescence proteins).

^aKU-KIST Graduate School of Converging Science and Technology, Korea University 145 Korea-ro, Seongbuk-gu, Seoul, Republic of Korea. E-mail: dklim@korea.ac.kr

^bDepartment of Biotechnology, College of Life Science and Biotechnology, Yonsei University, 50, Yonsei-ro, Seodaemun-gu, Seoul 120-749, Republic of Korea. E-mail: blseong@yonsei.ac.kr

† Electronic supplementary information (ESI) available. See DOI: [10.1039/c9ra09599c](https://doi.org/10.1039/c9ra09599c)



CA, USA). ATTO 565-Biotin dye was purchased from Sigma-Aldrich Co. (St. Louis, MO, USA) and Vivaspin 500 (pore size 0.2 μ m) was purchased from Sartorius Inc. (Göttingen, Lower Saxony, Germany).

Nickel-charged Sepharose columns (HisTrap HP 1) were purchased from GE Healthcare (Little Chalfont, UK). The buffer solutions such as 50 mM PBS (Phosphate Buffered Saline, pH 7.4, binding buffer), 10 mM PBS (pH 7.4, washing buffer), a tris buffer solution (50 mM tris(hydroxymethyl)aminomethane chloride (pH 7.5), 50 mM NaCl (sodium chloride), 1 mM DTT (dithiothreitol), 6 M guanidine-HCl and 0.1 mM EDTA (ethylene diamine tetraacetic acid, $\geq 99\%$), and buffer A (50 mM Tris-Cl (pH 7.5), 300 mM NaCl, 10% glycerol, 10 mM imidazole, 2 mM β -mercaptoethanol) and buffer B (50 mM Tris-Cl (pH 7.5), 300 mM NaCl, 10% glycerol, 300 mM imidazole, 2 mM β -mercaptoethanol) were obtained in dry powder form Sigma-Aldrich Co. (St. Louis, MO, USA). The plasmid (pGE-LysRS, a derivative of pGEMEX-1 (Promega Inc., Madison, WI, USA)) was used for the construction of plasmids for ht-GFP expression. *E. coli* strain (BL21 StarTM(DE3) pLysS) was purchased from Invitrogen (Carlsbad, CA, USA).

Instruments

The inverted type fluorescent microscope (Olympus IX71 Inc., Melville, NY, USA) equipped with 488 \times nm laser line and 20 \times objective was used for fluorescence intensity measurement. We used green filter sets (BP460-495 nm, BA510-550 nm) to detect excitation/emission wavelength.

The LSR II Flow cytometer analyzer¹⁸ (Becton Dickinson, San Jose, CA, USA) equipped with channel for Alexa Fluor 488 using a 525/50 BP (505SLP) filter (six colour detection) and channel for Cy5 using a 710/50 BP (685LP) filter and a series of hierarchical gates was applied to isolate single beads and analyzed the data with Denovo software (Los Angeles, CA, USA). The fluorescence intensity was monitored by a Cary Eclipse fluorescence spectrophotometer (Varian Inc., Springvale Road, Mulgrave, Australia).

The preparation of hexa-histidine and Tat fused GFP (ht-GFP)

HIV-1 transcription activator protein (Tat) containing enhanced green fluorescent (Tat-EGFP)¹⁹ and hexa histidine tag (ht-GFP) were used as model proteins. HIV Tat plasmid was constructed as following method. The HIV-1 Tat gene was selected from the HIV-1 complete genome (GenBank ID: NC_001802), chemically synthesized (GenScript, Piscataway, NJ, USA) and used as a template for PCR amplification. The forward primer was 5'-GGATCCATGGAGCCAGTAGATCCTAGACTAGAG-3' while the backward primer was 5'-GAATTCTTATTCGTGCCATTGATTT CTGAGCCTCGAAGATGTCGTTAG ACCCGCGG-3' (Cosmogene tech, Seoul, Republic of Korea).

The enhanced green fluorescent protein (EGFP) gene was amplified from plasmid, and inserted, using KpnI and SalI sites, into the end of the tat gene that was ligated into the NdeI and KpnI sites of pGE-LysRS, yielding ht-GFP. The oligonucleotide forward primer was: 5'-GGCACAAAGCTGGAGTACAAC-3' and the

reverse primer was 5'-ATGCCGTTCTGCTTGTC-3' for EGFP (Cosmogene tech, Seoul, Republic of Korea).

Expression and purification

The HIV-1 transcription activator protein Tat containing enhanced green fluorescent tagged His₆ (hexa histidines) (ht-GFPs) was expressed in *E. coli* strain. It was used as a host for protein expression. A hexa-histidine tag was added to the C-terminus of the protein for purification using nickel affinity chromatography. After adding 10 mL of a buffer A solution (50 mM Tris-Cl (pH 7.5), 300 mM NaCl, 10% glycerol, 10 mM imidazole and 2 mM β -mercaptoethanol) with 1 mM PMSF (phenylmethanesulfonyl fluoride) to the cells harvested from culture solution by centrifugation, the cells were suspended and lysed by sonication. The soluble fraction of lysates was loaded on the HisTrap HP1 column.¹⁴ After sufficient washing, the proteins were eluted under imidazole gradient from 10 mM to 300 mM by mixing buffer A and buffer B. The fractions were analysed by SDS-PAGE, using the buffer containing 50 mM Tris-Cl (pH 7.5), 50 mM NaCl, 1 mM DTT, and 0.1 mM EDTA.

Unfolding assay for ht-GFP quantification

The fluorescent intensity of the purified ht-GFP in PBS was measured at room temperature. The changes of fluorescence intensity were measured with time after urea treatment (6 M).

Agarose bead based assay procedures

Typically, the ht-GFP (*ca.* 1 μ g) was incubated with Ni-NTA agarose beads (30–50 of Ni-NTA agarose beads/10 μ L, protein binding capacity: 50 μ g) in the PBS buffer (50 mM, pH 7.4) (200 μ L). After shaking for 30 min at 4 °C, the Ni-NTA-agarose beads were washed twice with washing column buffer, then the fluorescent intensity of the agarose beads was measured.

Magnetic bead based assay using flow cytometry

The ht-GFP (*ca.* 1 μ g) was incubated with the binding buffer (50 mM PBS, pH 7.4) in 200 μ L and magnetic beads (30–50 of Ni-NTA agarose beads/10 μ L, protein binding capacity: 50 μ g) (Dynabeads[®] TALONTM). After shaking the mixture at 4 °C for overnight, the fluorescence intensity of magnetic bead solutions was measured without a washing step. The flow cytometer (BD LSR II) can detect Alexa Fluor 488 using a 525/50 BP (505SLP) filter and Cy5 with a 710/50 BP (685LP) filter, and a series of hierarchical gates were applied to isolate signals from single beads. The data were analyzed using FCS Express 5 from Denovo software (Los Angeles, CA, USA).

Results and discussion

Preparation and quantification of ht-GFP

To envision the capability of bead based assay for fluorescent protein quantification, we first prepared a green fluorescent protein (GFP) fused with hexa-histidine tag (His-6) at the C-terminus and HIV-1 transcription activator protein (Tat) at N-terminus as a model fluorescent protein. After expressing His-



6 and Tat fused green fluorescent protein (ht-GFP) in *E. coli*, ht-GFP was purified using nickel affinity chromatography. The analysis using polyacrylamide gel electrophoresis²⁰ showed a clear band of ht-GFP and the amount of ht-GFP could be estimated by comparing the band intensity with that of bovine serum albumin(BSA) as a standard (Fig. S1†). Then, three different methods such as fluorescence-based unfolding assay, agarose bead based assay with fluorescence microscopy, and magnetic bead based assay with flow cytometry were applied to compare their performance in determining the amount of ht-GFP.^{18,21-23}

The GFP protein consists of a structure containing a chromophore within Serine65-Tyrosine66-Glycine67 in a beta barrel that consists of 238 amino acids. The GFP protein slowly loosens its structure when exposed to urea, which induce the decrease of fluorescence intensity and the change can be measured with fluorometer.^{19,24} As shown in Fig. S2,† the native state fluorescence intensity of ht-GFP gradually decreased with time after the addition of urea (6.0 M) (called unfolding assay). By comparing the native state initial fluorescence intensity with the standard curve, the fluorescence intensity can be applied to determine the amount of ht-GFP.²⁵ But the initial fluorescence intensity *versus* the amount of ht-GFP is not linear and the fluorescence signal is not detectable in the low concentration of ht-GFP (<0.02 μ M), which is a major problem in determining the amount of ht-GFP solution (Fig. S2†).

Agarose bead based assay

To develop a sensitive and quantitative detection method for green fluorescent protein, we investigated a bead based simple quantification method using a Ni-NTA (nickel-nitrilotriacetic acid)-modified agarose bead particles (diameter: 45–165 μ m) (Scheme 1). The Ni-NTA modified agarose bead can immediately bind with the ht-GFP *via* the interactions between Ni-NTA and hexa-histidines in ht-GFP. It is believed that the protein structure is not denatured upon binding on the surface of the bead particle. Therefore, the fluorescent signal intensity from the ht-GFPs on the beads is closely related with the amount of native state ht-GFP. As shown in Fig. 1, the Ni-NTA beads alone showed no fluorescence signals, but the Ni-NTA-bead coupled with ht-GFP showed a strong fluorescence intensity. The sensitivity of the bead based ht-GFP detection method was investigated by mixing varying concentrations of ht-GFP (2.5 ng,

500 pg, 200 pg, and 50 pg) in 200 μ L binding buffer (50 mM PBS pH 7.4) and Ni-NTA-bead solution (10 μ L, protein binding capacity: 50 μ g). Then, the fluorescence signal intensity was monitored on the beads using fluorescence microscopy.²⁶ As shown in Fig. 1, the fluorescence intensity of ht-GFP gradually decreased with decrease in the amount of ht-GFP until the case of 50 pg incubation. The fluorescence intensity could be quantified by measuring the fluorescence intensity of individual bead particles as shown in Table S1.† The enriched state of ht-GFP on a bead is responsible for the excellent sensitivity of this method. In addition, the overall procedures are quite simple, rapid and easy to perform, which are also important factors for the direct quantification of fluorescent protein.

Flow cytometry for ht-GFP quantification

Furthermore, flow cytometry is more convenient and a quantitative way to measure fluorescence signal intensity.^{18,27} We also investigated the use of flow cytometry to quantify the amount of ht-GFP. Since the broad size distribution of agarose bead (45–165 μ m) is a limiting factor for flow cytometry, the use of bead with uniform size (1 μ m) with magnetic property is a desirable option because of low auto fluorescence background, higher sensitivity, and easy separation of bound protein.²⁸

To investigate such a performance, Ni-NTA magnetic beads combined with ht-GFP was analysed using flow cytometry (Fig. S3†). A dot plot provides the fluorescence intensities at Alexa Fluor 488 (positive control) on the X-axis and Cy5 (negative control) on the Y-axis. A quadrant marker divided the fluorescence parameter into four regions to distinguish populations that are considered negative, single positive, or double positive were measured (Fig. S3†). Using a quadrant marker, ht-GFP binding beads represents two fluorescence (Alexa Fluor 488 and Cy5) parameter plots into four sections to find out the percentages of ht-GFP binding populations (blue rectangle; Gate 2 mark region, bound ht-GFP protein) (Fig. S3†). A subclass control was used to determine the lower-left quadrant displays events that are negative for unbound ht-GFP protein (red rectangle; Gate 1 mark region, unbound ht-GFP protein) (Fig. S3†). The results indicated that the use of flow cytometry is a feasible way to measure the amount of target fluorescent protein after combining it with Ni-NTA magnetic bead.

Next, we investigated the sensitivity of magnetic bead based assay using flow cytometry. The Ni-NTA modified magnetic beads (1 mg μ L⁻¹) (protein detection capacity: approximately 10 μ g) were incubated with ht-GFP in binding buffer (50 mM PBS pH 7.4) for 30 min with varying amount of ht-GFP (0.5 ng–2.0 μ g), then the magnetic bead were analyzed using flow cytometry (Fig. 2c).¹⁷ The histogram in Fig. 2a indicated a big difference between 0 μ g and 0.5 μ g of ht-GFP. The increased population of fluorescence signal could be observed in the case of 1.0 and 2.0 μ g of ht-GFP incubation. The population of beads with green fluorescence signal was clearly identifiable from 0.6%, 92%, and 96.1% obtained from 0, 0.5, and 2.0 μ g of ht-GFP (Table S2†). Fig. 2b is the histogram obtained from the magnetic bead incubating low concentrations of ht-GFP (0.0–25 ng).

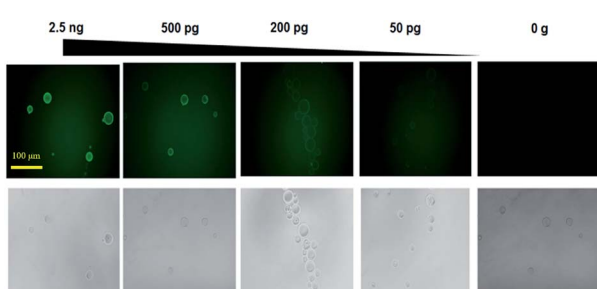


Fig. 1 The fluorescence images of bead obtained after incubating with ht-GFP (2.5 ng, 500 pg, 200 pg, 50 pg, and 0 g).



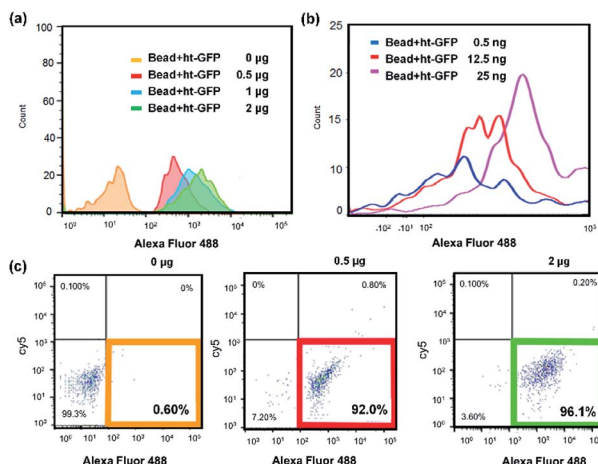


Fig. 2 Flow cytometry analysis for the magnetic beads incubated with varying amount of ht-GFPs (a) 0–2 µg, (b) 0.5–25 ng, (c) dot scattering plot (0–2 µg).

The histogram in Fig. 2b obtained from 0.5 ng and 12.5 ng of ht-GFP was partly overlapped with the histogram of negative control (0 µg of ht-GFP, Fig. 2a). However, the quadrant region analysis as shown in Fig. S4† clearly showed an increase in population of fluorescence beads even in case of 0.5 ng of ht-GFP (34%). The population of fluorescence signal linearly increased from 0% to 89% with increased amount (0–25 ng). Therefore, we can conclude that the detection limit of flow cytometry based method was 0.5 ng of ht-GFP, which is 2 order of higher detection limit than that of simple fluorescence microscopy based method. The flow cytometry is an automated method to accurately count the ht-GFP binding beads without sorting to eliminate unbound ht-GFPs. Therefore, the flow cytometry based method is more quantitative method that can detect high picogram ranges of fluorescent proteins than that of agarose bead based method. But in term of sensitivity, the Ni-NTA modified agarose bead based method is superior to flow cytometry based method.

Detection of native ht-GFPs in HeLa cells

Furthermore, the ultimate goal of bead-based method is the identification of the amount of ht-GFPs in native state directly from the cells without performing the purification step. To demonstrate such a possible application of Ni-NTA bead based method, we performed the Ni-NTA bead based fluorescence assay to identify the expression of native ht-GFPs in HeLa cells.

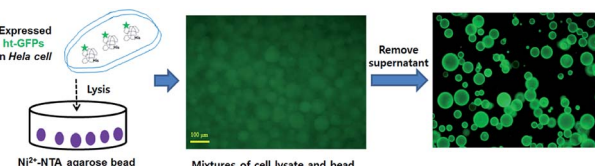


Fig. 3 The procedures of Ni-NTA bead based fluorescence images for the quantification of native ht-GFPs in HeLa cells.

The Ni-NTA beads were incubated with the lysates of HeLa cells to separate the expressed native ht-GFPs as shown in Fig. 3. The fluorescence image for the mixture of cell lysates and bead was not so clear because of high background fluorescence signal. However, after performing the washing step, the bead indicated a clear and bright fluorescence intensity (Fig. 3). By adding the mean value of the fluorescence intensity obtained from 1000 bead particles to the calibration curve equation, the amount of native ht-GFPs could be readily determined.

Conclusions

In summary, the results showed that a Ni-NTA bead based fluorescence measurement is a useful method in quantifying the amount of fluorescent protein without using additional enzyme-based assay.^{29,30} The enriched state of fluorescent protein on the bead through Ni-NTA binding affinity with histidine-rich protein and measurement of fluorescence are the essential parts for successful quantification with high sensitivity. Although the bead based assay require the calibration curve with purified fluorescent protein with histidine tags, once established, the method is very simple and straightforward to perform. This is useful method for complex proteomics studies and biomedical studies to identify potential target protein for various applications.^{31–34}

Conflicts of interest

There are no conflicts of interest to declare.

Acknowledgements

This research was supported by Basic Science Research Program and through the National Research Foundation of Korea (NRF) funded by the Ministry of Education (NRF-2018M3A9H4079358) and (NRF-2019R1I1A1A01043047). This work was also supported by a Korea University Grant, NRF-2017M3D1A1039421, and KU-KIST school research fund.

Notes and references

- 1 R. Y. Tsien, *Annu. Rev. Biochem.*, 1998, **67**, 509–544.
- 2 A. B. Chinen, C. M. Guan, J. R. Ferrer, S. N. Barnaby, T. J. Merkel and C. A. Mirkin, *Chem. Rev.*, 2015, **115**, 10530–10574.
- 3 N. C. Shaner, P. A. Steinbach and R. Y. Tsien, *Nat. Methods*, 2005, **2**, 905–909.
- 4 A. S. Mishin, V. V. Belousov, K. M. Solntsev and K. A. Lukyanov, *Curr. Opin. Chem. Biol.*, 2015, **27**, 1–9.
- 5 M. Kamiya and Y. Urano, *Curr. Opin. Chem. Biol.*, 2016, **33**, 9–15.
- 6 J. M. Kim, H. S. Choi and B. L. Seong, *RNA Biol.*, 2017, **14**, 926–937.
- 7 M. Chalfie, *Proc. Natl. Acad. Sci. U. S. A.*, 2009, **106**, 10073–10080.
- 8 J. A. Motyan, M. Miczi, B. Bozoki and J. Tozser, *Data Brief*, 2018, **18**, 203–208.



9 P. C. Liao, I. R. Boldogh, S. E. Siegmund, Z. Freyberg and L. A. Pon, *PLoS One*, 2018, **13**, e0196632.

10 A. L. Shapiro, E. Vinuela and J. V. Maizel Jr, *Biochem. Biophys. Res. Commun.*, 1967, **28**, 815–820.

11 K. Weber and M. Osborn, *J. Biol. Chem.*, 1969, **244**, 4406–4412.

12 A. Singh, D. Samanta, M. Boro and T. K. Maji, *Chem. Commun.*, 2019, **55**, 2837–2840.

13 A. Sedlmeier, A. Hlavacek, L. Birner, M. J. Mickert, V. Muhr, T. Hirsch, P. L. Corstjens, H. J. Tanke, T. Soukka and H. H. Gorris, *Anal. Chem.*, 2016, **88**, 1835–1841.

14 J. Crowe, H. Dobeli, R. Gentz, E. Hochuli, D. Stuber and K. Henco, *Methods Mol. Biol.*, 1994, **31**, 371–387.

15 A. Spriestersbach, J. Kubicek, F. Schafer, H. Block and B. Maertens, *Methods Enzymol.*, 2015, **559**, 1–15.

16 J. Wu, X. Wei, J. Gan, L. Huang, T. Shen, J. Lou, B. Liu, J. X. Zhang and K. Qian, *Adv. Funct. Mater.*, 2016, **26**, 4016–4025.

17 M. Dezfouli, S. Vickovic, M. J. Iglesias, P. Nilsson, J. M. Schwenk and A. Ahmadian, *Proteomics*, 2014, **14**, 14–18.

18 A. Adan, G. Alizada, Y. Kiraz, Y. Baran and A. Nalbant, *Crit. Rev. Biotechnol.*, 2017, **37**, 163–176.

19 G. S. Waldo, B. M. Standish, J. Berendzen and T. C. Terwilliger, *Nat. Biotechnol.*, 1999, **17**, 691–695.

20 A. Rath, M. Glibowicka, V. G. Nadeau, G. Chen and C. M. Deber, *Proc. Natl. Acad. Sci. U. S. A.*, 2009, **106**, 1760–1765.

21 H. Suarez, A. Gamez-Valero, R. Reyes, S. Lopez-Martin, M. J. Rodriguez, J. L. Carrascosa, C. Cabanas, F. E. Borras and M. Yanez-Mo, *Sci. Rep.*, 2017, **7**, 11271.

22 K. M. Ricks, N. M. Adams, T. F. Scherr, F. R. Haselton and D. W. Wright, *Malar. J.*, 2016, **15**, 399.

23 F. P. McManus, F. Lamoliatte and P. Thibault, *Nat. Protoc.*, 2017, **12**, 2342–2358.

24 A. Sacchetti and S. Alberti, *Nat. Biotechnol.*, 1999, **17**, 1046.

25 G. Reddy, Z. Liu and D. Thirumalai, *Proc. Natl. Acad. Sci. U. S. A.*, 2012, **109**, 17832–17838.

26 W. Cao, M. Chern, A. M. Dennis and K. A. Brown, *Nano Lett.*, 2019, **19**, 5762–5768.

27 A. Adan, G. Alizada, Y. Kiraz, Y. Baran and A. Nalbant, *Crit. Rev. Biotechnol.*, 2016, 1–14.

28 M. E. Materia, M. Pernia Leal, M. Scotto, P. B. Balakrishnan, S. Kumar Avugadda, M. L. Garcia-Martin, B. E. Cohen, E. M. Chan and T. Pellegrino, *Bioconjugate Chem.*, 2017, **28**, 2707–2714.

29 H. Du, X. Hu, H. Duan, L. Yu, F. Qu, Q. Huang, W. Zheng, H. Xie, J. Peng, R. Tuo, D. Yu, Y. Lin, W. Li, Y. Zheng, X. Fang, Y. Zou, H. Wang, M. Wang, P. S. Weiss, Y. Yang and C. Wang, *ACS Cent. Sci.*, 2019, **5**, 97–108.

30 A. Cernat, A. Le Goff, M. Holzinger, R. Sandulescu and S. Cosnier, *Anal. Bioanal. Chem.*, 2014, **406**, 1141–1147.

31 Y. Chen, Q. Cai and S. Liu, *Anal. Biochem.*, 2019, **587**, 113467.

32 J. C. Wang, H. Y. Ku, D. B. Shieh and H. S. Chuang, *Biomicrofluidics*, 2016, **10**, 014113.

33 L. Kahanovitz, E. Seker, R. S. Marks, M. L. Yarmush, T. Konry and S. J. Russell, *J. Diabetes Sci. Technol.*, 2016, **10**, 689–696.

34 M. W. Garbowski, Y. Ma, S. Fucharoen, S. Srichairatanakool, R. Hider and J. B. Porter, *Transl. Res.*, 2016, **177**, 19–30e15.

